Research Article

Efficient treatment of high-concentration sulfurous wastewater by using electrochemical oxidation process with Ti/SnO₂–Sb anode and air cathode

Shaoan Cheng[1] · Dan Xiao[1] · Yi Sun[1]

Abstract

High-concentration sulfurous wastewater is biologically toxic, corrosive, harmful to environment and human health, highly required to be separately treated. In this paper, an air–cathode electrochemical oxidation process (EO) was investigated to treat high-concentration sulfurous wastewater from coal chemistry industry. The effectiveness was evaluated by chemical oxygen demand (COD) removal, color (ADMI) removal, and total organic carbon (TOC) removal. The results showed that 99.1% COD, 100% color, and 94.5% TOC were removed by EO at the applied current of 40 mA cm^{-2} for 24 h. The COD removal accords with zero-order kinetics with a constant of 2598.3 mg L^{-1} h^{-1}, while the TOC removal follows the first-order kinetics with a constant of 0.1128 h^{-1}. The highest current efficiency of 94.3 ± 0.6% and the lowest energy consumption of 9.4 ± 0.1 kWh kg COD^{-1} were achieved when removing 98% of COD at the current density of 40 mA cm^{-2}. The results indicate that the air–cathode electrochemical oxidation process is feasible to efficiently treat high-concentration sulfurous wastewater.

1 Introduction

Sulfur-containing wastewater from industries such as refineries, chemical plants, and pharmaceutical plants is toxic, corrosive and with stink of sulfide or sulfur organics, posing a threat to the environment and human health [1, 2]. Different methods such as oxidation, neutralization, precipitation, gas stripping, etc., have been developed to treat this wastewater, depending on sources and concentrations of wastewater. However, the existing oxidation processes usually have low efficiency, the neutralization and gas stripping methods may cause secondary pollution due to the generation of SO₂, SO₃, and H₂S [2–5]. So a more efficient, safer but cheaper way should be developed for treating this wastewater.

The advanced oxidation processes (AOPs) generate high oxidizing substances such as hydroxyl radicals (·OH) and in situ oxidized contaminants at room temperature and atmosphere pressure [6–8], which are highly considered as environmental-friendly and effective technologies for treating refractory wastewater [6, 7, 9]. The AOPs mainly include photocatalytic oxidation, ozone oxidation, ultrasonic oxidation, electrochemical oxidation, Fenton oxidation, etc. [10, 11]. Among them, electrochemical oxidation (EO) process directly generates hydroxyl radicals on the anodes in situ oxidizing or mineralizing organic matters without requirement of adding other chemical agents [7, 12, 13]. EO receives more and more attention in the years due to its advantages of high efficiency, adaptability, good environmental compatibility and easy combination with other processes [14, 15].

EO has been investigated for treating various organic wastewaters like antibiotics [16], refineries [17, 18], dyes [19, 20], and insecticides [21]. The sulfur-containing wastewaters from coal chemical industries mainly contain sulfides, organic sulfur, polysulfides, and thiosulfate, which can all be oxidized as sulfate. Therefore, it is very likely practicable to use EO for treating high-concentration sulfurous wastewater especially when the wastewater has a high conductivity.

In this study, The EO process was investigated to treat real sulfur-containing wastewater. Ti/SnO$_2$–Sb electrodes were selected as anodes due to its easy preparation, low cost, and high catalytic oxidation activity, while air cathodes were selected as cathodes due to the possibility of making the system safer and more energy efficient [22–25]. The efficiency and kinetics were evaluated based on the COD removal, color removal, TOC removal, and energy consumption under different applied current densities.

2 Materials and methods

2.1 Sulfurous wastewater

Sulfurous wastewater was collected from the wet desulfurization of coal slurry gasification process in a local coal chemical factory (Zhejiang Fengdeng chemical Co., Ltd.). The wastewater is in dark green color and smells with mild stink. The typical characteristics of the sulfurous wastewater used in this study are shown in Table 1. The wastewater was stored in a refrigerator at 4 °C before use.

Table 1 Typical characteristics of the sulfurous wastewater

Items	Values
pH	8.69–9.27
Conductivity (m S cm^{-1})	110 ± 10
Chemical oxygen demand, COD (mg L^{-1})	51100 ± 2000
Ammonia nitrogen (mg L^{-1})	180 ± 10
Sulfate (mg L^{-1})	19000 ± 100
Sulfide (mg L^{-1})	<0.005
Thiosulfate (mg L^{-1})	9800 ± 100
Chloride (mg L^{-1})	11000 ± 100
ADMI (unit PtCo)	15500 ± 500
Total N (mg L^{-1})	280 ± 10
Total organic carbon, TOC (mg L^{-1})	2150 ± 10

2.2 Electrolytic cell and operation

2.2.1 Preparation of Ti/SnO$_2$–Sb anode

The Ti/SnO$_2$–Sb anodes were prepared by coating antimony-doped tin oxide (SnO$_2$–Sb) on the surface of a titanium sheet as following procedures: (1) Titanium sheets (2 × 2 cm) were first sanded with 400 mesh and 800 mesh of sandpapers, then degreased in a solution of 40% NaOH for 30 min at 80 °C, and followed by etching in a 10% oxalic acid solution for 2 h. (2) SnO$_2$–Sb was coated on Ti sheet by four steps as: firstly immersing the sheets in the solution consisting of 8.76 g of SnCl$_4$·5H$_2$O and 0.091 g of SbCl$_3$ and 25 mL of isopropanol and then taking the sheets out from the solution and drying at 100 °C for 10 min, following by calcining the sheets in a muffle furnace at 520 °C for 10 min; (2) Repeat procedure for 9 times, (3) and finally calcine the resulted sheet at 550 °C for 1 h.

2.2.2 Preparation of air–cathode

The stainless-steel air cathodes, composing of a catalytic layer, a stainless-steel mesh collector, and a gas diffusion layer, were prepared according the method reported [26]. Stainless-steel mesh was firstly soaked in a 15% ethanol solution for 24 h. The diffusion layer was prepared as following steps: (1) Polytetrafluoroethylene (PTFE) and carbon black (CB) of mass ratio 2:3 were firstly mixed in 60% PTFE emulsion to form a viscous paste after stirring, ultrasonically shaking, and heating. (2) Press the paste to a 1.5-mm-thick circle and heat at 100 °C for 2 h. (3) The circle was finally pressed to the side of the stainless-steel mesh and followed by heating at 340 °C for 30 min. The catalytic layer was prepared as follows: (1) Activated carbon (AC) and carbon black (CB) of mass ratio 10:1 were mixed into isopropanol following by stirring and ultrasonically shaking until it becomes viscous [27]. (2) The mixture was pressed to a circle with a thickness of 1.0 mm and followed by heating at 120 °C for 2 h. (3) The circle was pressed to another side of the stainless-steel mesh and followed by heated at 200 °C for 30 min.

2.2.3 Electrolytic cell and operation

The electrolytic cell is rectangular parallelepiped with an overall size of 7 cm*5 cm*5 cm. There is a cylindrical chamber with a diameter of 3 cm and a height of 6 cm inside. The reactor was equipped with double cathodes and double anodes. Two anodes (size of 2 cm*2 cm) were in middle with a spacing of 2 cm and two cathodes (size

of 7 cm^2) were on both sides at a distance of 6 cm and contacted with air.

The two cathodes were connected to the negative pole of a direct current power source (E3649A, Agilent, USA) using a wire, while the two anodes were to the positive pole. The experiments were operated in galvanostatic and batch mode under different current densities ranged from 20 to 50 mA cm^{-2}, sampled at a certain interval for COD and ADMI measurement. The potential of anodes and cathodes were collected by a data acquisition instrument (34970A, Agilent, USA), while Ag/AgCl electrodes were used as reference. Current efficiencies (CE) and energy consumptions (EC) at different current density were calculated, and the optimal current density was identified. Besides that, LSV, UV–Vis, and TOC tests were also conducted under optimal current density to further analyze the mechanism of anodic oxidation of sulfurous wastewater. The experiments under different current densities were repeated at least three times and the results were averaged. Error bars were used to reflect the standard deviation of the results.

2.3 Analysis methods

Current efficiencies (CE) were calculated according to Eq. (1), and energy consumption (EC) was according to Eq. (2)

$$CE = \frac{FbV_s\Delta COD}{MIt} \times 100 \tag{1}$$

$$EC = \frac{UIt}{3600V_g\Delta COD} \tag{2}$$

where F is Faraday constant (96485 C mol^{-1}), V_s is the volume of solution (L), b is the number of electron transfer, M is relative molecular mass (here M is the O_2 molecular weight of 32 g mol^{-1}), ΔCOD is the change of COD concentration (g L^{-1}), I is the applied current (A), t is time (h), U is the cell voltage (V).

In order to analyze the degradation mechanism of the electrochemical oxidation process, the zero-order and first-order kinetic models were used to analyze the concentration changes of COD and TOC. The zero-order model is [28]:

$$\frac{d(COD_t)}{dt} = K_1 \tag{3}$$

where K_1 is a zero-order kinetic constant (mg L^{-1} h^{-1}); COD_t is the COD concentration of sulfurous wastewater at time t (mg L^{-1}).

The first-order kinetic model is [12]:

$$\ln\left(\frac{TOC_0}{TOC_t}\right) = K_2 \cdot t \tag{4}$$

where K_2 is first-order kinetic constant (h^{-1}), TOC_t is the TOC concentration at time t (mg L^{-1}), TOC_0 is the original TOC concentration of sulfurous wastewater (mg L^{-1}), t is the time (h).

Besides, COD was determined using spectrophotometric methods according to the procedure (DR2800, HACH, USA), and TOC measurements were conducted in Muti N/C 3100 TOC analyzer. Ammonia nitrogen was tested by Nessler's reagent spectrophotometry, and chloride, sulfide, sulfate, and thiosulfate were measured by ion chromatography(Integrity, Thermo Fisher Scientific, USA). ADMI is a method for evaluating true colors set by the American Dye Manufacturer's Institute. The water samples were measured by glass cuvette with a light path of 1 cm, using a HACH DR2800 built-in ADMI standard curve (wavelength 455 nm). Conductivity was measured by portable conductivity meter (F3-Standard Kit, METTLER TOLEDO, China). The UV–Vis spectra were obtained using a UV spectrophotometer (N5000, YOKE INSTRUMENT, China) with the scanning range from 190 to 1100 nm. The linear sweep voltammetry (LSV) were carried out on an electrochemical work station (CHI660D, CHENHUA, China) in the potential range of 0–3 V at scan rate of 5 mV s^{-1}.

3 Results and discussion

## 3.1 Effect of current density on COD and color removal

COD removal depended on the different current densities (Fig. 1a). At the current density of 20 mA cm^{-2}, the COD removal was only 60.5% (from 51100 to 20200 mg L^{-1} in average) after 64 h of electrolysis. When current density increased to 30 mA cm^{-2}, the COD removal increased to 98.6% (from 51100 to 720 mg L^{-1} in average) within 40 h. Further increased current density to 40 mA cm^{-2}, the COD removal increased to 99.1% of (from 51100 to 483 mg L^{-1} in average) in only 24 h. The COD concentration linearly decreased with the operation time as a zero-order kinetics (Fig. 1a). The kinetics constant K_1 according to Eq. (3) increased from 481.3 to 2953.5 mg·L^{-1}·h^{-1} when the current density increased from 20 to 50 mA cm^{-2} (Fig. 1b). It should be noted that the kinetics constant of COD removal slowly increased when the current density was over 40 mA cm^{-2}.

The color removal changed with the current densities in same path as the COD (Fig. 2a). At the current density of 20 mA cm^{-2}, the color removal was only 78.2% (from 15600 to 3400 in average) after 64 h of electrolysis. When

Fig. 1 The effect of current density on COD. **a** COD concentration as a function of electrolysis time and **b** kinetic constants K_1 at current density of 20 mA cm^{-2}, 30 mA cm^{-2}, 40 mA cm^{-2}, 50 mA cm^{-2}
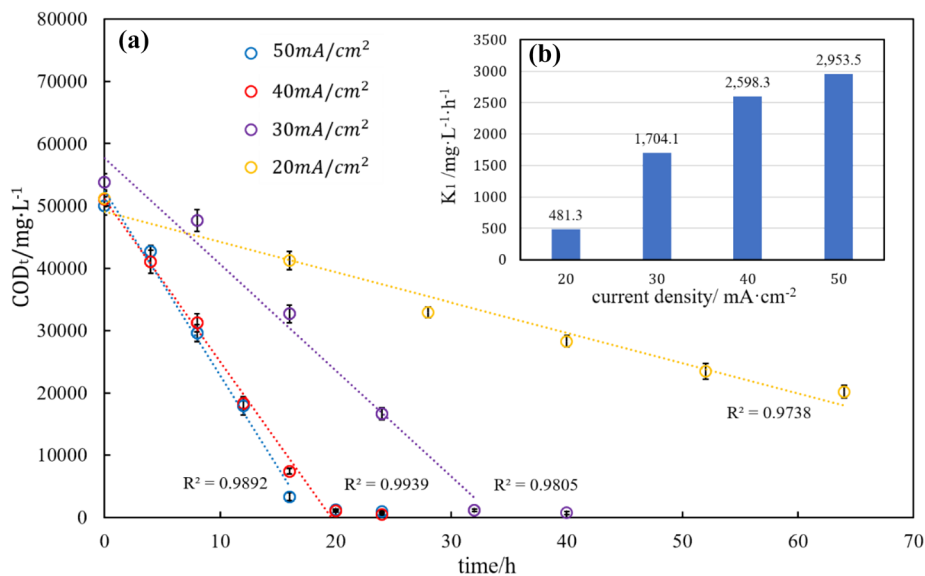
Fig. 2 The effect of current density on color removal. **a** Residual color as a function of electrolysis time at current density of 20mA cm^{-2}, 30 mA cm^{-2}, 40 mA cm^{-2}, 50 mA cm^{-2}. **b** The comparison of before (left) and after (right) electrolysis of 24 h at 40 mA cm^{-2}
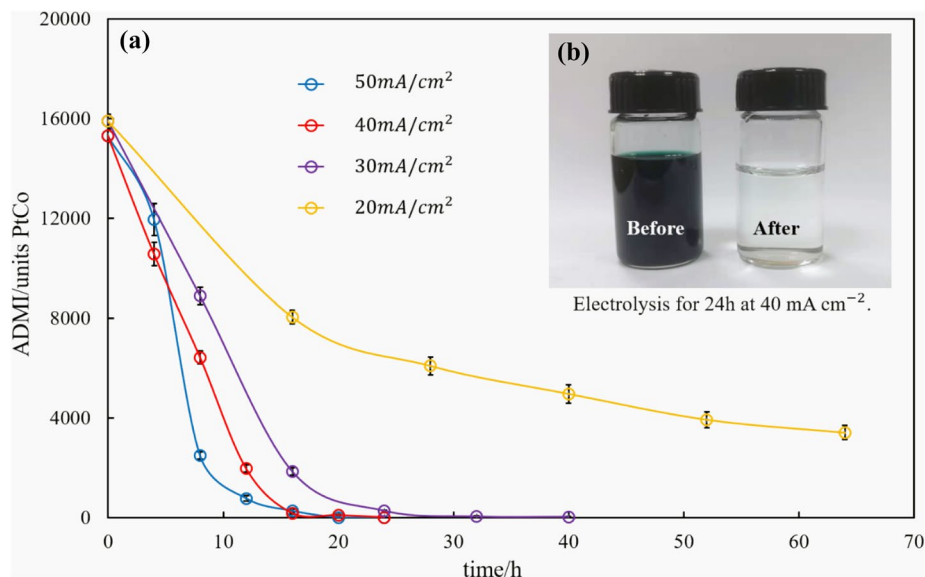
current density increased to 30 mA cm^{-2}, the color can be almost completely removed with 99.9% color removal within 40 h (from 15600 to 20 in average). The color was completely removed within 24 h when the current density further increased to over 40 mA cm^{-2}. The comparison of wastewater before and after electrolysis at current density of 40 mA cm^{-2} for 24 h is shown in Fig. 2b.

3.2 Effect of current density on current efficiency (CE) and energy consumption (EC)

Current efficiency (CE) and energy consumption (EC) were calculated according to Eqs. (1) and (2) under different current densities when removal is about 98% COD, and the results are given in Table 2. The highest CE of 94.3 ± 0.6%

Table 2 Effect of current density on CE and EC. CE and EC at current densities of 30 mA cm^{-2}, 40 mA cm^{-2}, and 50 mA cm^{-2} when removed 98% COD

Current density (mA cm^{-2})	COD removal (%)	CE (%)	EC (kWh·kg COD^{-1})
30	98	82.7 ± 0.5	10.1 ± 0.1
40	98	94.3 ± 0.6	9.4 ± 0.1
50	98	61.6 ± 0.2	21.1 ± 0.1

and the lowest EC of 9.4 ± 0.1 kWh·kg COD^{-1} were obtained when current density was 40 mA cm^{-2}. At current densities of 30 mA cm^{-2} and 50 mA cm^{-2}, the CE and EC were 82.7 ± 0.5%, 10.1 ± 0.1 kWh·kg COD^{-1} and 61.6 ± 0.2%, 21.1 ± 0.1 kWh·kg COD^{-1}, respectively.

Energy consumption of wastewater treatment cannot be simply compared since it depends on many factors like wastewater sources, concentration, pH, and applied current density, etc. And there are few studies focusing on treating the sulfurous wastewater by electrochemical oxidation methods at present. Therefore, some other industrial actual wastewater treatment studies using electrochemical oxidation were selected for qualitative comparison of energy consumption. Zou et al. used EO process equipping BDD anode to treat real textile wastewater. When adjusted initial pH to 2 and added 3 g L^{-1} NaCl reagent, the lowest EC of 11.12 kWh·kg COD^{-1} was obtained [29]. Wang et al. combined EO technology with biological aerated filter for advanced treatment of biotreated coking wastewater. At the current density of 75 mA cm^{-2} and HRT of 45 min, the COD was removed from 221.2 to 113.5 mg L^{-1}, and the EC was calculated as 67.9 kWh·kg COD^{-1} [30]. Zhu et al. obtained EC of 64 kWh·kg COD^{-1} when also conducted study of advanced treatment of biologically pretreated coking wastewater using EO process [31]. Comparing with these results, our system performed much lower of energy consumption. Two reasons are likely for this low EC: One is the introduction of air cathodes, and another is the high conductivity of sulfurous wastewater. In this system, the using of air cathodes increased the average potential of cathodes by 0.910 V (from -1.493 to -0.583 V) at the current density of 40 mA cm^{-2}, which was equivalent to reducing voltage by 24.9%. In this high cathode potential, part of O_2 could be reduced to H_2O_2 at air cathodes, and the generation of H_2O_2 was beneficial for oxidation of contaminants and intermediates [25]. The sulfurous wastewater used had a high conductivity of 110 ± 10 mS cm^{-1} which lowered the resistance and therefore the energy consumption [32].

It can be observed the anode potentials mainly depended on the COD concentration, but the cathode potentials apparently influenced by current densities, which indicated that cathode potentials were the main factor affecting the EC at different current densities (as Fig. 3). When current density was increased from 30 to 40 mA cm^{-2}, the average cathode potential slightly decreased from -0.415 V to -0.583 V, and the EC at these two current densities were close likewise. With a further increase in the current density to 50 mA cm^{-2}, the average cathode potential significantly reduced to -1.064 V together with great increase in EC to 21.1 ± 0.1 kWh kg COD^{-1}. The significant decrease in cathode potentials may because the oxygen diffusion and reduction rate of the air cathodes are limited by electrode structure, and the stronger polarization will occur and lower the cathode potential rapidly when continuously increase the current density. Consequently, comprehensively considering the COD removal, color removal, current efficiency, energy consumption, and time cost, 40 mA cm^{-2} can be considered as the optimal current density.

3.3 Mineralization of organics

TOC concentrations at optimum current density of 40 mA cm^{-2} are presented in Fig. 4a. TOC, the total organic carbon, represents the amount of carbon-containing organic compounds in the solution. As shown in Fig. 4a, the TOC concentration decreased gradually and reduced to 118 mg L^{-1} from 2150 mg L^{-1} after 24 h (removal of 94.5%), which indicated that Ti/SnO_2–Sb anodes can efficiently mineralize the organics in wastewater. The first-order kinetic can perfectly fit to the TOC degradation with r^2 of 0.9959 and K_2 of 0.1228 h^{-1} (as Fig. 4b). Besides that,

Fig. 3 The effect of current density on CE and EC. Anode potential (above 0 V) and air cathode potential (below 0 V, vs Ag/AgCl) as a function of COD removal at the current density of 30 mA cm^{-2}, 40 mA cm^{-2} and 50 mA cm^{-2}
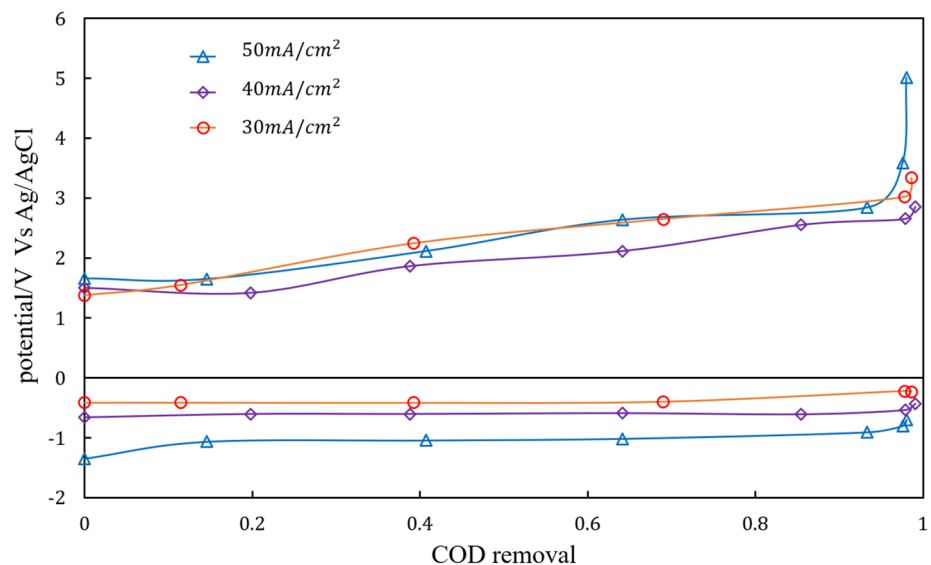
Fig. 4 TOC concentration as a function of electrolysis time at current density of 40 mA cm^{-2}
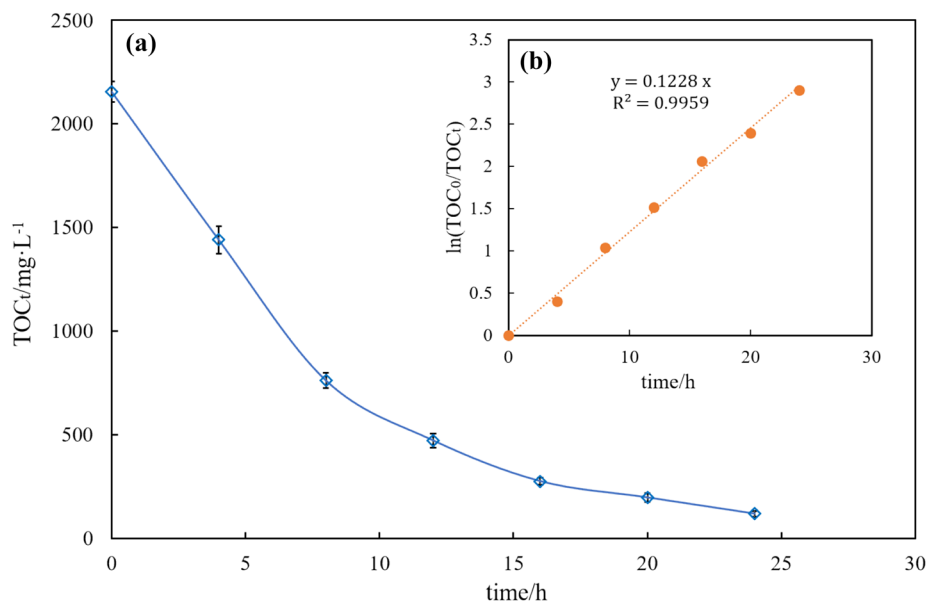
the concentration of sulfate increased from 19000 ± 100 to $189,800 \pm 100$ mg L^{-1} after 24 h of electrolysis, indicating that sulfur compounds in wastewater were also fully oxidized.

GC–MS tests were conducted to identify the species in sulfurous wastewater. Like the general characteristic of coal chemical wastewater, the composition of wastewater was extremely complicated. According to the results of GC–MS, more than 30 species were detected in wastewater, including sulfur-containing substances, aliphatic hydrocarbons and derivatives, and aromatics and derivatives. Some representative species are listed in Table 3. Considering that the wastewater was produced in a wet desulfurization process and sulfur as by-product, the synthesis of polysulfide organic compounds such as dimethyl tetrasulfide was unavoidable. The existing organic sulfur can explain the high COD but low TOC concentration (COD: 51100 ± 2000 mg L^{-1}, TOC: 2150 ± 10 mg L^{-1}). The detected S_8 was most likely the residual of the sulfur by-product suspending in wastewater. Therefore, the increase in sulfate from 19000 ± 100 mg L^{-1} to 189800 ± 100 mg L^{-1} was due to the oxidation of these sulfur-containing substances. In addition, the detection of more than 20 types of aliphatic hydrocarbons and their derivatives and three types of aromatics illustrated the attribution of TOC and 94.5% removal of TOC indicated the mineralization of these organics.

The UV–Vis spectrums at optimum current density are shown in Fig. 5, and there are 5 peaks appearing at 194 nm, 215 nm, 608 nm, 675 nm, and 817 nm. Since the absorption spectrums of the organics are closely related to the measurement conditions, such as solvent, temperature, and pH, and due to the presence of various species

in wastewater, we cannot precisely determine the attribution of these absorption peaks. Results of GC–MS tests manifested that there were aliphatic hydrocarbons and derivatives, aromatics and derivatives and polysulfide existing in the wastewater. Generally, the absorption peaks of alkane molecules appear in the far ultraviolet region ($\lambda < 200$ nm), and the presence of a heteroatom substitution and an unsaturated bond would cause a redshift, so the peaks at 194 nm and 215 nm were presumed to be aliphatic hydrocarbon substances or derivatives thereof. The peaks at 608 nm, 675 nm, and 817 nm were highly likely to be absorption peaks of polysulfides, and when the number of sulfur atoms in the polysulfide increases, the polysulfide absorption peaks gradually move toward to infrared region [33–35]. It can be seen in Fig. 5 that the absorbance of these peaks gradually weakened with the electrolysis. After 24 h, these five absorption peaks completely disappeared or weaken significantly, indicating the degradation of these characteristic substances.

3.4 Anodic oxidation mechanisms

LSV curves tested at different time at optimal current density of 40 mA cm^{-2} are shown in Fig. 6. The anodizing current gradually decreased during the first 16 h of electrolysis and then did not change significantly anymore at the last 8 h. Electrochemical oxidation of pollutants takes place through two different mechanisms: direct anodic and indirect anodic oxidation. The continuous recession of oxidation current at first 16 h might be caused by the decrement of pollutants in wastewater, manifesting the occurrence of direct anodic oxidation process which means electrons were directly transferred

Table 3 Representative species in wastewater detected by GC–MS including the substances, retention time (t_R), chemical formula, and mass spectrogram
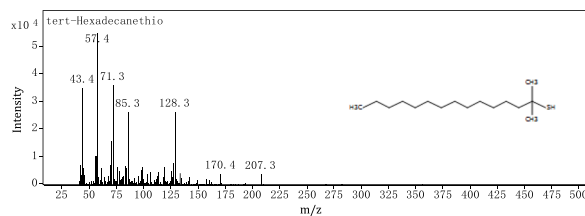
Sulfur-containing species
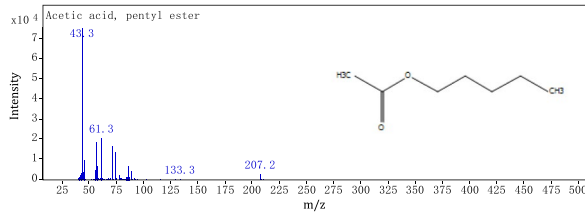
Dimethyl Tetrasulfide
t_R=12.584 min, $C_2H_6S_4$
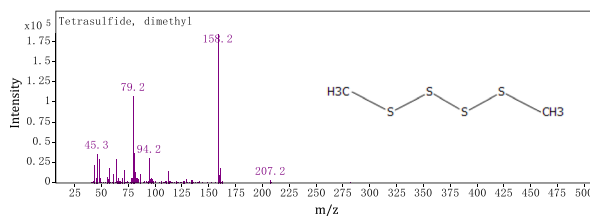
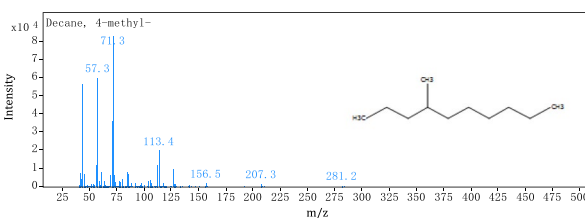

Cyclic Octaatomic sulfur
tR =25.162 min, S_8
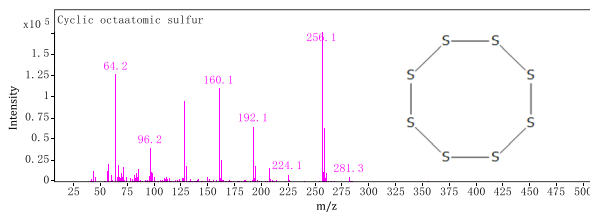
Tert-Hexadecanethiol
t_R =12.308 min, $C_{16}H_{33}SH$
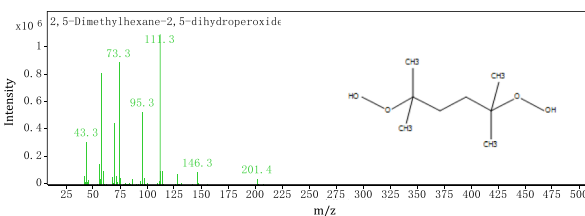

Aliphatic hydrocarbons and derivatives

Pentyl acetate
t_R=5.180 min, $C_7H_{14}O_2$
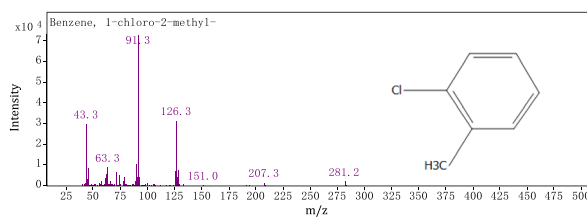

4-methyl-Decane
t_R=9.163 min, $C_{11}H_{24}$

2,5-Dimethylhexane-2,5-dihydroper
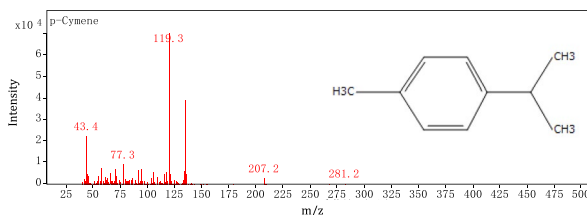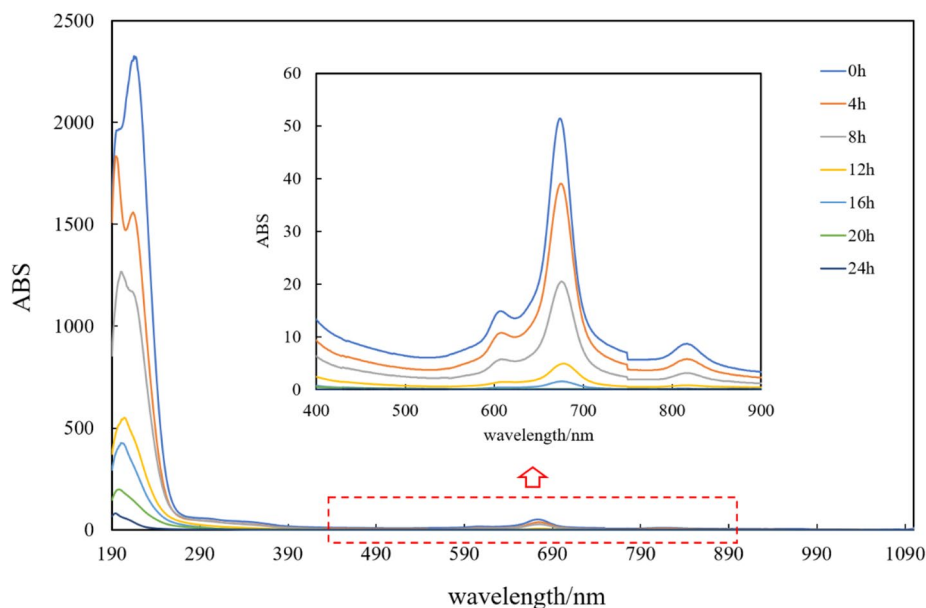oxide
t_R=9.163 min, $C_8H_{18}O_4$

Table 3 (continued)

Aromatics and derivatives

1-chloro-2-methyl-Benzene

t_R =7.855 min, C_7H_7Cl

p-Cymene

t_R =11.427 min, $C_{10}H_{14}$

Fig. 5 UV–Vis spectrum analysis (scanning range from 190 to 1100 nm, current density of 40 mA cm^{-2})

from the contaminants to the anodes. The taking place of direct oxidation can explain the high CE obtained under this system to some extent. In the last 8 h, the anodizing current had no significant change, but the COD concentration continued to decrease (Fig. 1a), indicating the occurrence of indirect oxidation. For the indirect oxidation, in addition to the contribution of hydroxyl radicals (·OH), the chlorine (Cl_2) and hypochlorous acid/hypochlorite (HClO/ClO^-) would also be produced at the anodes because of the existing of 11000±100 mg L^{-1} Chloride (Cl^-) in wastewater. Hypochlorous acid reacts with unsaturated bonds and electron-rich moieties (reduced sulfur moieties, and aromatics) [8]. Furthermore, Ti/SnO_2–Sb anodes surface can also generate ozone (O_3) [36] which also helps to

degrade the pollutants. So the COD degradation in the last 8 h can be attributed to the indirect oxidation of ·OH, Cl_2, HClO/ClO^-, and O_3.

4 Conclusions

The electrochemical oxidation system combining Ti/SnO_2–Sb anodes and air cathodes can be used to efficiently treat high-concentration sulfurous wastewater. COD removal of 99.1%, chroma removal of 100%, and TOC removal of 94.5% were achieved at the optimum current density of 40 mA cm^{-2} in 24 h. The system performed a high current efficiency of 94.3±0.6% and low

Fig. 6 Liner voltammetry analysis. Anode as working electrode, cathode as counter electrode and Ag/AgCl as reference electrode, the effluent treated by different time as the electrolyte, scanning range 0–3 V and scanning rate 5 mV s^{-1}, current density 40 mA cm^{-2}
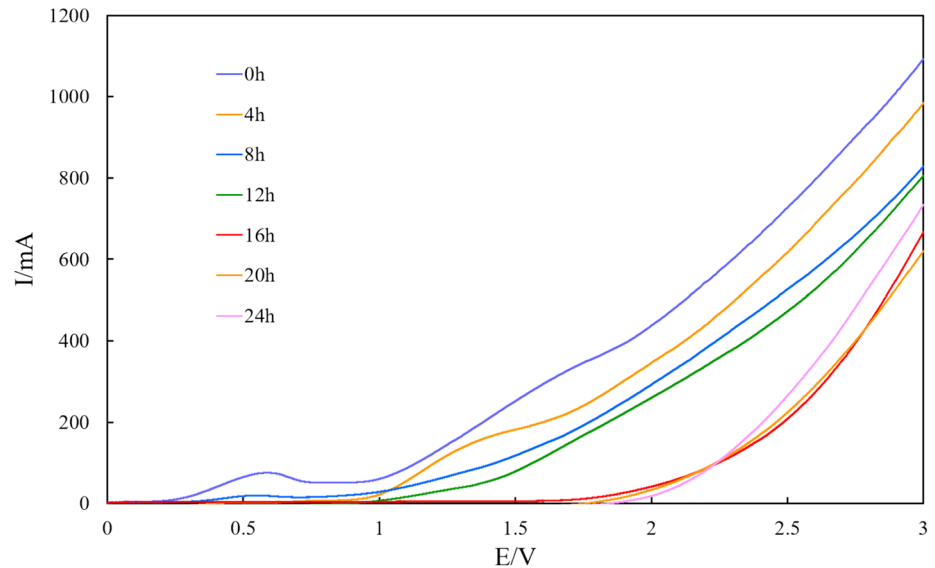
energy consumption of 9.4 ± 0.1 kWh·kg COD^{-1} due that the average electrolysis voltage was significantly reduced by air–cathodes application. The mechanism of electrochemical oxidation in this system is likely the combination of direct and indirect anodic oxidation.

Compliance with ethical standards

Conflict of interest The author(s) declares that they have no competing interests

References

1. Joshi DR, Zhang Y, Gao Y, Liu Y, Yang M (2017) Biotransformation of nitrogen- and sulfur-containing pollutants during coking wastewater treatment: correspondence of performance to microbial community functional structure. Water Res 121:338–348
2. Pokasoowan C, Kanitchaidecha W, Bal Krishna KC, Annachhatre AP (2009) Investigation on laboratory and pilot-scale airlift sulfide oxidation reactor under varying sulfide loading rate. J Environ Sci Health, Part A 44(1):87–98
3. Ma SF, Wang CL, Liu AH, Guo YJ, He HL (2007) Experimental study on treatment of high-concentrated sulfur wastewater by process of depositing natrojarosite and its environmental significance. Acta Geol Sin English Ed 81(2):330–334
4. Wu M, Wang Z, Zhou J, Niu M, Jiang X, Lv Y, Xiao Q, Li G, Wang Y (2018) Release characteristics and control of hydrogen sulfide during thermal drying of municipal wastewater sludge. J Mater Cycles Waste Manage 20(2):946–954
5. Ding L, Liu T, Li X (2014) Removal of CH$_3$SH with in situ generated ferrate (VI) in a wet-scrubbing reactor. J Chem Technol Biotechnol 89(3):455–461
6. Wang JL, Xu LJ (2012) Advanced oxidation processes for wastewater treatment: formation of hydroxyl radical and application. Crit Rev Environ Sci Technol 42(3):251–325
7. Oturan MA, Aaron J (2014) Advanced oxidation processes in water/wastewater treatment: principles and applications: a review. Crit Rev Environ Sci Technol 44(23):2577–2641
8. Radjenovic J, Sedlak DL (2015) Challenges and opportunities for electrochemical processes as next-generation technologies for the treatment of contaminated water. Environ Sci Technol 49(19):11292–11302
9. Tijani JO, Fatoba OO, Madzivire G, Petrik LF (2014) A review of combined advanced oxidation technologies for the removal of organic pollutants from water. Water Air Soil Pollut 225(9):2102
10. Comninellis C, Kapalka A, Malato S, Parsons SA, Poulios I, Mantzavinos D (2008) Advanced oxidation processes for water treatment: advances and trends for R&D. J Chem Technol Biotechnol 83(6):769–776
11. Ahmed MB, Zhou JL, Ngo HH, Guo W, Thomaidis NS, Xu J (2017) Progress in the biological and chemical treatment technologies for emerging contaminant removal from wastewater: a critical review. J Hazard Mater 323:274–298
12. Zhou MH, Wu ZC, Ma XJ, Cong YQ, Ye Q, Wang DH (2004) A novel fluidized electrochemical reactor for organic pollutant abatement. Sep Purif Technol 34(1–3):81–88
13. Anglada N, Urtiaga A, Ortiz I (2009) Contributions of electrochemical oxidation to waste-water treatment: fundamentals and review of applications. J Chem Technol Biotechnol 84(12):1747–1755
14. Sirés I, Brillas E (2012) Remediation of water pollution caused by pharmaceutical residues based on electrochemical separation and degradation technologies: a review. Environ Int 40:212–229
15. Lin H, Niu J, Xu J, Huang H, Li D, Yue Z, Feng C (2013) Highly efficient and mild electrochemical mineralization of long-chain perfluorocarboxylic acids (C$_9$-C$_{10}$) by Ti/SnO$_2$–Sb–Ce, Ti/SnO$_2$–Sb/Ce–PbO$_2$, and Ti/BDD electrodes. Environ Sci Technol 47(22):13039–13046
16. Antonin VS, Santos MC, Garcia-Segura S, Brillas E (2015) Electrochemical incineration of the antibiotic ciprofloxacin in sulfate medium and synthetic urine matrix. Water Res 83:31–41

17. Wei L, Guo S, Yan G, Chen C, Jiang X (2010) Electrochemical pre-treatment of heavy oil refinery wastewater using a three-dimensional electrode reactor. Electrochim Acta 55(28):8615–8620

18. Yan L, Ma H, Wang B, Wang Y, Chen Y (2011) Electrochemical treatment of petroleum refinery wastewater with three-dimensional multi-phase electrode. Desalination 276(1–3):397–402

19. Brillas E, Martínez-Huitle CA (2015) Decontamination of waste-waters containing synthetic organic dyes by electrochemical methods. An updated review. Appl Catal B 166–167:603–643

20. Nidheesh PV, Zhou M, Oturan MA (2018) An overview on the removal of synthetic dyes from water by electrochemical advanced oxidation processes. Chemosphere 197:210–227

21. Borràs N, Arias C, Oliver R, Brillas E (2011) Mineralization of desmetryne by electrochemical advanced oxidation processes using a boron-doped diamond anode and an oxygen-diffusion cathode. Chemosphere 85(7):1167–1175

22. Sun Z, Zhang H, Wei X, Du R, Hu X (2015) Fabrication and elec-trochemical properties of a SnO_2–Sb anode doped with ni-nd for phenol oxidation. J Electrochem Soc 162(9):H590–H596

23. Li XY, Cui YH, Feng YJ, Xie ZM, Gu JD (2005) Reaction pathways and mechanisms of the electrochemical degradation of phenol on different electrodes. Water Res 39(10):1972–1981

24. Shao D, Liang J, Cui X, Xu H, Yan W (2014) Electrochemical oxida-tion of lignin by two typical electrodes: Ti/Sb–SnO_2 and Ti/PbO_2. Chem Eng J 244:288–295

25. Yu H, Li Y, Zhao M, Dong H, Yu H, Zhan S, Zhang L (2015) Energy-saving removal of methyl orange in high salinity wastewater by electrochemical oxidation via a novel Ti/SnO_2-Sb anode-Air diffusion cathode system. Catal Today 258:156–161

26. Dong H, Yu H, Wang X, Zhou Q, Feng J (2012) A novel structure of scalable air-cathode without Nafion and Pt by rolling activated carbon and PTFE as catalyst layer in microbial fuel cells. Water Res 46(17):5777–5787

27. Zhang X, Xia X, Ivanov I, Huang X, Logan BE (2014) Enhanced activated carbon cathode performance for microbial fuel cell by blending carbon black. Environ Sci Technol 48(3):2075–2081

28. Kim J, Nam Y, Yu J, Song J (2014) Simultaneous removal of odour-ous and organic compounds in septic tanks using an electrolytic oxidation system. Desal Water Treatment 52(4–6):929–936

29. Zou J, Peng X, Li M, Xiong Y, Wang B, Dong F, Wang B (2017) Electrochemical oxidation of COD from real textile wastewa-ters: kinetic study and energy consumption. Chemosphere 171:332–338

30. Wang CR, Hou ZF, Zhang MR, Qi J, Wang J (2015) Electrochemi-cal oxidation using BDD anodes combined with biological aer-ated filter for biotreated coking wastewater treatment. J Chem 2015:1–7

31. Zhu X, Ni J, Lai P (2009) Advanced treatment of biologically pre-treated coking wastewater by electrochemical oxidation using boron-doped diamond electrodes. Water Res 43(17):4347–4355

32. Dominguez CM, Oturan N, Romero A, Santos A, Oturan MA (2018) Removal of lindane wastes by advanced electrochemi-cal oxidation. Chemosphere 202:400–409

33. Patel MUM, Demir-Cakan R, Morcrette M, Tarascon J, Gaberscek M, Dominko R (2013) Li–S battery analyzed by UV/Vis in oper-ando mode. Chemsuschem 6(7):1177–1181

34. Patel MUM, Dominko R (2014) Application of in operando uv/vis spectroscopy in lithium-sulfur batteries. Chemsuschem 7(8):2167–2175

35. Gobeltz N, Ledé B, Raulin K, Demortier A, Lelieur JP (2011) Syn-thesis of yellow and green pigments of zeolite LTA structure: identification of their chromophores. Microporous Mesoporous Mater 141(1–3):214–221

36. Cheng S, Chan K (2004) Electrolytic generation of ozone on an antimony-doped tin dioxide coated electrode. Electrochem Solid-State Lett 7(3):D4–D6